$\Omega_{\rm M}$ and Ω_Λ from 11 SNe Ia Observed with WFPC-2 on HST

R. A. Knop and the Supernova Cosmology Project

Received _____; accepted _____

to be submitted to *The Astrophysical Journal*

ABSTRACT

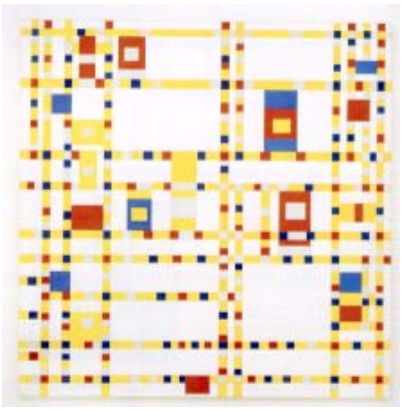

1. Introduction

TO BE WRITTEN

2. Observations, Data Reduction, and Lightcurve Fits

The supernovae discussed in this paper are listed in Table 1. They were discovered during three different supernova searches similar to those described in Perlmutter *et al.* (1999). Two of the searches were conducted at the 4m Blanco telescope at the Cerro Tololo Inter-American Observatory (CTIO), in December 1997 and March/April 1998. The final search was conducted at the Canada-France-Hawaii Telescope (CFHT) on Mauna Kea in Hawaii in April/May 2000. Each supernova was discovered in a two-epoch search. Images were acquired at two epochs separated by 3-4 weeks. Images from the first epoch were subtracted from images from the second epoch; residual signals represented supernova candidates. Spectra obtained at the 10m Keck and 8m VLT observatories (and ESO 3.6m? check this) confirmed the identification of the candidates as SNe Ia, and measured the redshift of each candidate. Where possible, the redshift z of each candidate was measured

by matching narrow features in the host galaxy of the supernovae; the precision of these measurements in z is typically 0.001. In cases where there were not sufficient host galaxy features, redshifts were measured from the supernova itself; in these cases, z is only precise to typically 0.01. However, even in the latter case redshift measurements are precise enough so as to be dwarfed by photometric errors.

Each of these supernovae was followed with two broadband filters with the Wide Field/Planetary Camera 2 (WFPC2) on the Hubble Space Telescope (HST). Table 1 lists the dates of these observations. The two filters were chosen to be those closest to the ground-based R-band (F675W) and I-band (F814W) filters. These filters correspond to redshifted B- and V-band filters for supernovae at $z < 0.7$, and redshifted U- and B- band filters for supernovae at $z > 0.7$. Each listed observation comprises at least two images taken within the same orbit, split for purposes of cosmic ray rejection. In some cases (the longer exposures), a single observation is the sum of more than two images.

The HST images were reduced through the standard HST data reduction pipeline (ACONLEY– HELP ME OUT HERE, ANYTHING MORE TO SAY?). Photometric fluxes ☑ were extracted from the final images using a PSF-fitting procedure. Traditional PSF fitting procedures assume a single isolated point source above a constant background. In this case, the point source was superimposed on top of the image of the host galaxy. In all cases, the supernova image was separated from the core of the host galaxy; however, in most cases the separation was not enough that an annular measurement of the background would be accurate. Because the host galaxy flux should be constant in all of the images, we used a PSF fitting procedure which fit a PSF *simultaneously* to every image of a given supernovae observed through a given photometric filter. The model we fit was:

$$f_i(x,y) = f_{0i} * \mathrm{psf}(x - x_{0i}, y - y_{0i}) + \mathrm{bg}(x - x_{0i}, y - y_{0i}; a_j) + z_i \qquad (1)$$

Table 1: Supernova Observations

SN Name	z	F675W Observations	F814W Observations
1997ek	0.863	1998-01-05 (800s)	1998-01-05 (1200s)
		1998-01-11 (800s)	1998-01-11 (1200s)
			1998-02-02 (2300s)
			1998-02-14 (2300s)
			1998-02-27 (2300s)
			1998-11-09 (2400s)
			1998-11-16 (2400s)
1997eq	0.538	1998-01-06 (600s)	1998-01-06 (600s)
		1998-01-21 (800s)	1998-01-11 (1200s)
			1998-02-02 (1200s)
		1998-02-11 (800s)	1998-02-11 (1200s)
		1998-02-19 (800s)	1998-02-19 (1200s)
1997ez	0.778	1998-01-05 (800s)	1998-01-05 (1200s)
		1998-01-11 (800s)	1998-01-11 (1200s)
			1998-02-02 (2300s)
			1998-02-14 (2300s)
			1998-02-27 (4600s)
9878	0.644	1998-04-08 (600s)	1998-04-08 (600s)
		1998-04-19 (600s)	1998-04-19 (600s)
		1998-04-30 (800s)	1998-04-30 (1200s)
		1998-05-15 (800s)	1998-05-15 (1200s)
		1998-05-28 (800s)	1998-05-28 (1200s)
1998as	0.355	1998-04-08 (800s)	1998-04-08 (1200s)
		1998-04-20 (800s)	1998-04-20 (1200s)
		1998-05-11 (800s)	1998-05-11 (1200s)
		1998-05-15 (800s)	1998-05-15 (1200s)
		1998-05-29 (800s)	1998-05-29 (1200s)
1998aw	0.440	1998-04-08 (600s)	1998-04-08 (600s)
		1998-04-18 (600s)	1998-04-18 (600s)
		1998-04-29 (800s)	1998-04-29 (1200s)
		1998-05-14 (800s)	1998-05-14 (1200s)
		1998-05-28 (800s)	1998-05-28 (1200s)
1998ax	0.497	1998-04-08 (600s)	1998-04-08 (600s)
		1998-04-18 (600s)	1998-04-18 (600s)
		1998-04-29 (800s)	1998-04-29 (1200s)
		1998-05-14 (800s)	1998-05-14 (1200s)
		1998-05-27 (800s)	1998-05-27 (1200s)
1998ay	0.638	1998-04-08 (800s)	1998-04-08 (1200s)
		1998-04-20 (800s)	1998-04-20 (1200s)
			1998-05-11 (2300s)
			1998-05-15 (2300s)
			1998-06-03 (2300s)
1998ba	0.430	1998-04-08 (600s)	1998-04-08 (600s)
		1998-04-19 (600s)	1998-04-19 (600s)
		1998-04-29 (800s)	1998-04-29 (1200s)
		1998-05-13 (800s)	1998-05-13 (1200s)
		1998-05-28 (800s)	1998-05-28 (1200s)
1998bi	0.740	1998-04-06 (800s)	1998-04-06 (1200s)
		1998-04-18 (800s)	1998-04-18 (1200s)
			1998-04-28 (2300s)
			1998-05-12 (2300s)
			1998-06-02 (2300s)
2000fr	0.543		2000-05-08 (2200s)
		2000-05-15 (1200s)	2000-05-15 (1200s)
		2000-05-28 (1200s)	2000-05-28 (1200s)
		2000-06-10 (1000s)	2000-06-10 (800s)
		2000-06-22 (2400s)	2000-06-22 (2300s)
		2000-07-08 (2400s)	2000-07-08 (2300s)

where $f_i(x, y)$ is the measured flux in pixel (x, y) of the ith image, f_{0i} is the total flux in the supernova in the ith image, psf(u, v) is a normalized point spread function, bg(u, v) is a constant background parametrized by a_j, and z_i is a pedestal offset for the ith image. There are $4n + m - 1$ parameters in this model, where n is the number of images (typically 2, 5, or 6 summed images) and m is the number of parameters a_j that specifies the background model (typically 3 or 6). The -1 is due to the fact that a zeroth-order term in the background is degenerate with one of the z_i terms. The model was fit to 7×7 or 9×9 patches extracted from all of the images of a time sequence of a single candidate in a single filter.

A single Tiny Tim PSF, corrected by an empirical electron diffusion term Fruchter (2000), was used for all images of a given band. Although this is an approximation– the PSF of WFPC2 depends on the epoch of the observation as well as the position on the chip– this approximation should be a good one. All of the supernovae were positioned close to the center of the chip. To verify that this approximation was valid, we reran the PSF fitting procedure with individually generated PSFs for most supernovae; the measured fluxes were not significantly different.

Fluxes extracted in this manner were corrected for the charge transfer efficiency (CTE) of WFPC-2 following the procedure of Dolphin (2000) (updated by the coefficients posted later on the author's web page– how do I cite this). Because the galaxy background is a smooth background underneath the point source, it was considered as a contribution to the background in the CTE correction. For an image which was a combination of several separate exposures within the same orbit or orbits, the CTE calculation was performed assuming that each image had a measured flux whose fraction of the total flux was equal to the fraction of that individual image's exposure time to the summed image's total exposure time.

Ground-based photometric fluxes were extracted from images using the same aperture photometry procedure of Perlmutter *et al.* (1999). A complete lightcurve in a given filter (R or I) combined the HST data with the ground-based data, using measured zeropoints for the ground based data and the Vega zeropoints of Dolphin (2000) for the HST data. An uncertainty of 0.02 was assumed for all HST zeropoints; this uncertainty was added as a correlated error between all HST data points when combining with the ground-based lightcurve. Similarly, the measured uncertainty in the ground-based zeropoint was added as a correlated error to all ground-based fluxes.

Color corrections were performed iteratively. An initial fit was performed simultaneously to the R and I band lightcurves (see below). This fit was interpolated to produce an R-I color at each epoch on the lightcurve. This R-I color was used with empirical linear color terms (which are typically small, of order 0.01) for each ground based telescope, and with second-order color terms from Dolphin (2000) for the HST data. The difference between the Bessel R and F675W filters, and between the Bessel I and F814W filters, made the HST color corrections were significant. Moreover, the difference between the spectral energy distribution (SED) of a supernova and of a star with the same R-I color were significant ($\geq 10\%$ for some R-F675W corrections). The fit to the lightcurve produced a time of maximum, lightcurve width, and R-I color. The supernova coordinates together with the dust maps of Schlegel *et al.* (1998) produced a estimate of E(B-V) due to dust within the Galaxy. A template SN Ia spectrum (see below) corresponding to the z, epoch relative to B-max, lightcurve width, measured galactic E(B-V), and with a host E(B-V) necessary to produce the measured R-I color was integrated to produce this additional color correction.

At each iteration, the R and I lightcurves are re-fit to a template supernova, and the color corrections re-applied, until the fit converges.

The assumed SED used for color corrections is based on the master SN Ia template

spectrum generated by Nugent *et al.* (2002) from a library of low-redshift SN Ia spectra. This template was adjusted so that it produced the observed integrated BVRI colors at each epoch of a normal SN Ia. These observed colors were derived by interpolating the lightcurves for low redshift supernovae published in Hamuy (1996) and Riess (1999). Points were interpolated from the lightcurve of each supernova from these papers, where there was data within 4 days of a given epoch relative to rest-B maximum (corrected for cosmological $(1+z)$ time dilation); these points were plotted as a function of the fit stretch value (see below) of the supernova. A ridge line in these plots of B-V, V-R, and R-I vs. stretch defined the fiducial $z = 0$ BVRI colors at each epoch as a (weak) function of stretch. When extracting a spectrum for use in color corrections or K-corrections, the template spectrum of the appropriate epoch, $(t - t_{max})/(s(1+z))$, has its colors adjusted first for stretch, then for any specified E(B-V) extinction, then for redshift, then for specified Galactic E(B-V) extinction.

The lightcurve model fit to the supernova had four parameters: time of rest-B maximum of the lightcurve, peak flux in R, R-I color, and stretch s. Stretch (Goldhaber 2001) is a parameter which multiplies the time axis of the lightcurve, so that a supernova with a high stretch has a relatively slow decay from maximum, and a supernova with a low stretch has a relatively fast decay from maximum. For supernovae in the redshift range $z = 0.3$–0.7, a B template was fit to the R-band lightcurve and a V template was fit to the I-band lightcurve. For the three supernovae at $z > 0.7$, a U template was fit to the R-band lightcurve and a B template to the I-band lightcurve. The B template used was that of Goldhaber (2001), and the U template was the same as that used by Perlmutter *et al.* (1999). For this paper, a new V-band template was generated from the nearby supernova lightcurve data of Hamuy (1996) and Riess (1999). This V-band template was generated simultaneously with stretch-based fits to the B-band lightcurves of the same nearby supernovae, so that the generated V template was for a $s = 1$ supernova, and was

optimized for stretch-based fits. This V-band template was a spline under tension with 10 control points located between 12 days before and 80 days after maximum light, and an additional 4 control points between 80 and 320 days after maximum; the fit parameters were the vertical (flux) position of the control points.

Each lightcurve fit used K-corrections following the procedure used in Perlmutter *et al.* (1999).

QUESTION: Should we tabulate the actual lightcurve data? ☑

3. Results and Discussion: Magnitudes and Colors

Table 2 lists the peak R magnitudes, R-I colors, and stretches from the lightcurve fits, in addition to the redshift z and the Galactic extinction E(B-V) for each of the supernovae in this paper. In addition is listed a rest-frame peak B magnitude, which was calculated from an observed magnitude by adjusting it for Galactic extinction using $A_X(z)$, and by applying the proper K-correction. The rest-frame peak B magnitude has not been corrected for host galaxy E(B-V) extinction. $A_X(z)$ was based on the extinction law of O'Donnell (1994), and was adjusted for the SED of a SN Ia template spectrum (see Section 2). $A_R(z)$, for example, varies from 2.76 to 2.54 for light coming into the Galaxy from a SN Ia at redshifts between 0 and 0.95.

The tabulated peak B magnitude (plus the effects of host galaxy extinction and any stretch/luminosity correction) is what will be used as a standard candle magnitude for cosmological fits; see Section 4. For supernovae with $0.3 < z < 0.7$, the observed R peak magnitude was K-corrected to the rest-B magnitude, and for supernovae with $z > 0.7$ the observed I peak magnitude was K-corrected to the rest-B magnitude. $A_X(z)$ was based on the extinction law of O'Donnell (1994), and was adjusted for the SED of a SN Ia template

spectrum (see Section 2). $A_R(z)$, for example, varies from 2.76 to 2.54 for light coming into the Galaxy from a SN Ia at redshifts between 0 and 0.95.

In addition, Table 2 lists a predicted R-I color, and a host galaxy E(B-V) value. The predicted R-I color is the R-I color at rest-B maximum expected based on integration of the template spectrum described in Section 2 for a supernova of the appropriate z, stretch s, and Galactic E(B-V). E(B-V) is the sum of the difference between the measured R-I color and the predicted R-I color, and the difference in the K-corrections ($K_{BR} - K_{VI}$ or $K_{UR} - K_{BV}$; Rob, check the sign of these based on standard conventions). ☑

Table 2: Supernova Magnitudes and Colors I

SN	z	s	E(B-V)$_{MW}$	m$_R$	m$_B$	R-I	R-I$_{\rm pred}$	E(B-V)$_{\rm host}$
1998as	0.355	0.88(2)	0.037			0.29(4)	0.05	0.26
1998ba	0.430	0.88(2)	0.024			0.17(4)	0.04	0.13
1998aw	0.440	1.01(2)	0.026			0.37(4)	0.06	0.32
1998ax	0.497	1.02(3)	0.035			0.21(4)	0.15	0.07
1997eq	0.538	0.95(3)	0.044			0.19(4)	0.22	-0.03
2000fr	0.543	1.03(1)	0.030			0.12(4)	0.22	-0.11
1998ay	0.638	1.02(5)	0.035			0.35(7)	0.45	-0.13
(9878)	0.644	0.73(3)	0.029			0.49(6)	0.44	0.05
1998bi	0.740	1.01(3)	0.026			0.51(5)	0.69	-0.25
1997ez	0.778	1.04(1)	0.026			0.65(6)	0.80	-0.22
1997ek	0.863	1.07(6)	0.042			0.76(7)	1.07	-0.43

The most striking feature visible in Table 2 is the disparity between the measured R-I and predicted R-I values. If the measured R-I is higher (redder) than the predicted R-I, there is a natural explanation: extinction in the host galaxy of the supernova has reddened the spectrum, resulting in a positive E(B-V) which must be taken into account when using this supernova as a standard candle. However, especially for supernovae at higher redshifts, the measured values of R-I are systematically *bluer* than the predicted values of R-I. The

most reasonable explanation is that there is something wrong with the predicted values.

While the fiducial BVRI colors of a SN Ia are well measured from the low-redshift SN Ia lightcurve data published by Hamuy (1996) and Riess (1999), there is not at the moment as much high-quality data on the U-B color of a low redshift supernova. Knowledge of the U-B color is important for accurate predictions of values of R-I measured from higher redshift supernovae. At $z > 0.7$, where the rest U-band K-corrects to the observed R band, this is obvious. Even at lower redshifts such as $0.50 < z < 0.65$, where the observed R filters overlaps more with a redshifted B than an redshifted U filter, there is substantial "contamination" of the observed R light by light blueward of what is measured through a B filter from a SN Ia at $z = 0$. Consequently, accurate R-I predictions require a template spectrum which has been scaled to have a proper U-B color in addition to proper BVRI colors. The measured R-I colors for high-redshift supernovae are bluer than the predicted colors, suggesting that our template has a weaker flux in U relative to B than it should have.

The template spectrum used to generate K-corrections and color corrections, as well as values of $\mathrm{R\text{-}I_{pred}}$ in Table 2, had a U-B color of -0.22 at the epoch of B maximum (Branch 1996). Henceforth we shall describe this template as the "U-suppressed" template. SN 1994D was a supernova which was a normal Type Ia, except that it was brighter in the U-band that expected for a SN Ia by ~ 0.3 magnitudes (Mielke 1996). We generated a new template spectrum, following the procedure described in Section 2, adjusted to have the same BVRI colors as the U-suppressed template, but with the U-B color decreased by 0.3 magnitudes everywhere along the lightcurve. From this "U-enhanced" template, we performed a new set of supernovae lightcurve fits; because the template in use affects the color and K-corrections, it is necessary to repeat the lightcurve fit and color correction iteration procedure described in Section 2. Table 3 shows the results of these fits, together

with the R-I_{pred} and E(B-V)$_{host}$ values calculated from the U-enhanced template.

Table 3: Supernova Magnitudes and Colors II

SN	z	s	E(B-V)$_{MW}$	m_R	m_B	R-I	R-I_{pred}	E(B-V)$_{host}$
1998as	0.355	0.89(2)	0.037			0.28(4)	0.14	0.14
1998ba	0.430	0.90(2)	0.024			0.14(4)	0.08	0.06
1998aw	0.440	1.00(2)	0.026			0.31(4)	0.09	0.23
1998ax	0.497	1.05(3)	0.035			0.20(4)	0.12	0.08
1997eq	0.538	0.93(3)	0.044			0.19(4)	0.14	0.06
2000fr	0.543	1.04(1)	0.030			0.08(3)	0.14	-0.06
1998ay	0.638	0.98(4)	0.035			0.31(7)	0.23	0.10
(9878)	0.644	0.72(3)	0.029			0.51(6)	0.21	0.36
1998bi	0.740	1.00(3)	0.026			0.47(5)	0.40	0.10
1997ez	0.778	1.03(1)	0.026			0.62(6)	0.50	0.16
1997ek	0.863	1.07(6)	0.042			0.75(7)	0.76	-0.02

The values in this table produce better agreement between predicted and measured values of R-I at higher redshifts; there is no longer a problem with a significant number of supernovae being "too blue".

Histograms of the E(B-V) color excess distributions for this set of supernovae and for those from Hamuy (1996) and Perlmutter *et al.* (1999) are plotted in Figure 1. Although the fitting procedure used for the previously published sets is the same as that used in Perlmutter *et al.* (1999) for those supernovae, all supernovae have been re-fit using the new V template of this paper (see Section 2); in addition, the $z > 0.1$ SNe from Perlmutter *et al.* (1999) were fit using K-corrections calculated with both the U-suppressed and U-enhanced template spectra. (We verified that we obtained identical confidence regions on the $\Omega_M - \Omega_\Lambda$ plane using the magnitudes for the supernovae from Perlmutter *et al.* (1999) obtained from these redone fits.) Finally, although values of E(B-V) were determined in a value equivalent to the method of determination used in Perlmutter *et al.* (1999), slightly different values of

the assumed unreddened BVRI colors were used for this paper (see Section 2). Note that for cosmological purposes, the parameters Ω_M and Ω_Λ are determined by the curvature of the m_B vs. z curve; as such, the $z < 0.1$ supernovae are effectively used to establish a linear slope, and the high-redshift supernovae are used to determine the deviation from an empty universe. For this reason, the absolute values of E(B-V) are not as important as the *difference* between the average E(B-V) for the two different sets (low redshift and high redshift) of supernovae. If the same excess rest-frame extinction correction A_B is applied to both sets, it will affect any measured value of the Hubble constant (or, equivalently, of the absolute magnitude of a SN Ia), but not the measurements of Ω_M or Ω_Λ.

The top panel (a) of Figure 1 shows the values of E(B-V) determined for the 18 supernovae from Hamuy (1996) which form the low-redshift sample defined by Perlmutter *et al.* (1999). The central panels (b and c) show the values of E(B-V) determined for those high-redshift supernovae from Perlmutter *et al.* (1999) which have color measurements available. Panel b plots E(B-V) values calculated from predicted R-I colors with the U-suppressed template, and panel c calculated predicted R-I colors with the U-enhanced template. Panels d and e show the histogram of E(B-V) for the HST-observed supernovae reported in this paper; again, the left and right panels show, respectively, predicted values of R-I calculated with he U-suppressed and U-enhanced templates. On each of the four lower panels, the solid line is the distribution which would be observed if the E(B-V) values plotted in the top panel for the low-z supernovae were the true values, but were observed with the distribution error bars in R-I of the high-redshift set. In other words, if the distribution of physical values of E(B-V) were identical for the low-redshift set of supernovae and one of the high-redshift sets of supernovae, the histogram and solid line should be aligned. The solid line does *not* directly indicate the uncertainties in R-I or in E(B-V) for a given set, but rather those uncertainties convolved with the distribution in panel a.

The distribution show in panel (b) differs slightly from the histogram in Figure 6b of Perlmutter *et al.* (1999) for two reasons. First, the supernovae were refit with the new V-template, possibly yielding slightly different values of R-I. Second, this paper uses slightly different *predicted* values of R-I, which propagate into slightly different values of E(B-V) in a manner which is a weak function of redshift. Most importantly, this paper does not distinguish between points based on their E(B-V) uncertainty, and it includes supernovae whose rest R-I more closely matches U-B than it does B-V. (NOTE: Even though the 42SNe paper claims not to include U-B points in the E(B-V) histogram, I think it does! Check this.) The best comparison between this histogram and that of Figure 6b of Perlmutter *et al.* (1999) would be to compare this figure to the full histogram, including boxes of all shading, in the previous work. The solid line in this figure and the dashed line in the previous work are normalized differently; the previous work normalized the area of the solid line to the area of the shaded boxes, whereas this work normalizes the area of the solid line to the full area of all supernovae in the histogram.

It is apparent in Figure 1 that the high-redshift E(B-V) distribution better matches what would be predicted from the low-redshift E(B-V) distribution if a U-enhanced template is used to predict the R-I colors than if a U-suppressed template is used. This difference is particularly striking in the current set of supernovae, which have redshifts more or less uniformly distributed between 0.35 and 0.86; in contrast, the majority of the supernovae in Perlmutter *et al.* (1999) were at $z \sim 0.5$. The difference between R-I colors predicted from the two different template spectra becomes more pronounced with increasing redshift. This suggests that the U-enhanced template spectrum is a better approximation to the true average SN Ia spectrum observed in both high-redshift sets than the U-suppressed template. Indeed, a comparison of the histograms in panels (c) and (e) with the solid line suggests that a greater fraction of the current set of supernovae suffer from mild but significant E(B-V) extinction than was the case in Perlmutter *et al.* (1999); however, this number only

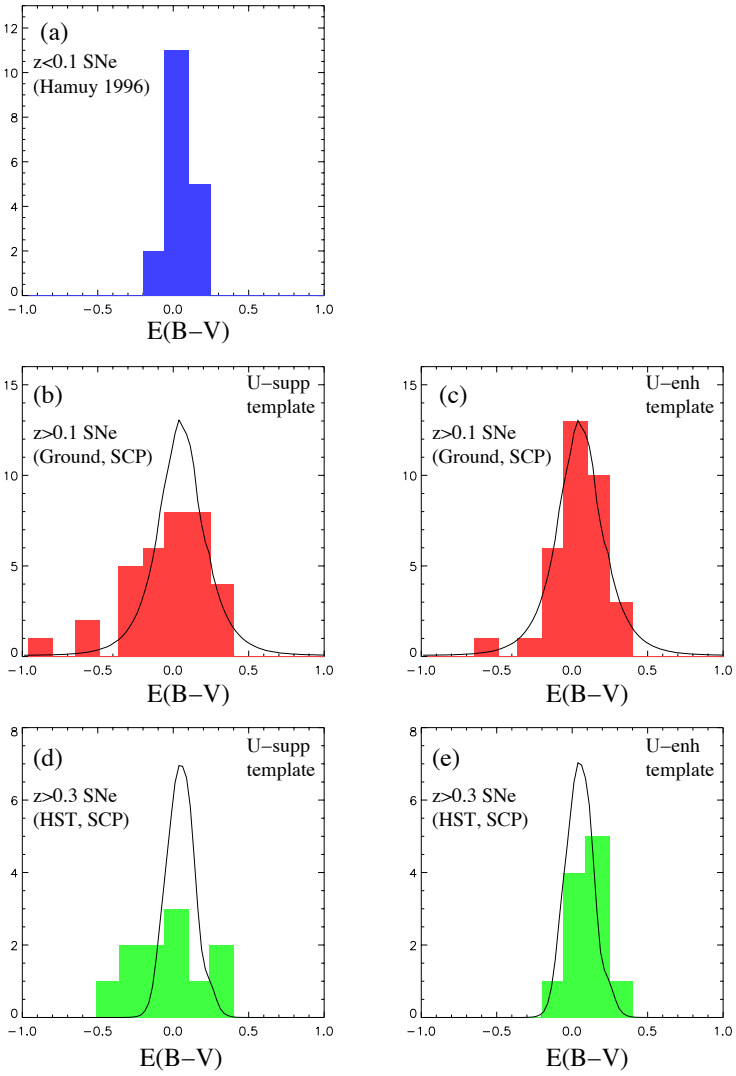

Fig. 1.— Host galaxy E(B-V) histograms. galaxy. Panel (a) shows E(B-V) for the 18 low-z supernovae from Hamuy (1996). Panels (b) and (c) show E(B-V) for the 42 supernovae from Perlmutter *et al.* (1999), refit using the new V-template of this paper. Panels (d) and (e) show E(B-V) or the 11 HST SNe of this paper. E(B-V) was calculated from the difference between the observed R-I and the R-I color predicted from a template spectrum, given the values of z, s, and Milky Way E(B-V). Panels (b) and (d) use R-I colors predicted from the U-suppressed template; panels (c) and (e) use R-I colors predicted from the U-enhanced template. The solid line on panels (b) through (e) show the distribution that would be expected from a sample of supernovae whose true E(B-V) distribution is that of panel (a), but which were observed with the distribution uncertainties in E(B-V) appropriate for each panel (b) through (e).

amounts to two or three out of the total small set of eleven supernovae.

The fact that the U-enhanced template better predicts the colors of the high-redshift supernovae than the U-suppressed template is *not* evidence for supernova evolution. At the moment, it is primarily the result of the fact that our knowledge of the "true" U-B color of a SN Ia is uncertain. While there is a wealth of BVRI on low-redshift SNe Ia available, there is very little high quality published U-band data on such supernovae. Consequently, the true distribution of peak U-band absolute magnitudes for SNe Ia is poorly understood. The U-suppressed template may be no more representative of even the low-redshift sample of supernovae than the U-enhanced template. Second, even if there is a difference in the observed peak U magnitudes of the low and high redshift supernovae (for which we have no evidence), it does not necessarily indicate evidence for evolution of the supernova population. Most of the high-redshift searches were conducted in the R-band, and as such would be more sensitive to supernovae which are overluminous in the U-band (cite Nugent on this?). If the distribution of absolute U magnitudes is intrinsically broader than the distribution of absolute B magnitudes, then these supernovae will still be satisfactory standard candles in the B-band, even if they are overluminous in U. Note that at the highest redshifts (which are those supernovae with the greatest leverage on Ω_M and Ω_Λ), the rest-B band magnitudes are estimated from observed I-band magnitudes, which is the filter that best overlaps the redshifted B filter.

The U-suppressed template was used to determine the cosmological results of Perlmutter *et al.* (1999), but here we suggest that perhaps the U-enhanced template might produce better results. However, the differences that the two templates have upon the calculated supernova magnitudes *do not change the cosmological conclusions of Perlmutter et al. (1999)*. The calculated values of Ω_M and Ω_Λ are not very sensitive to which template is used, see Section 4. The vast majority of this sensitivity comes from mis-estimates of

E(B-V) due to a "too blue" template, rather than the effect of the different SED templates on the K-corrections. None of the supernovae which passed the "Case C" criteria in Perlmutter *et al.* (1999) (which omitted supernovae with significant evidence for reddening) would have been omitted using the U-enhanced template; thus, the different SED template would only very mildly affect their Case C results. (Probably this should be shown and quantified!) Section 4 shows that the effect of the different SED templates on E(B-V) do visibly shift the Ω_M/Ω_Λ confidence regions, although the shift is less than half of the width of those regions (corresponding to a $\sim 1-\sigma$ shift). √

Although calculated values of E(B-V) are sensitive to the template, thereby affecting an extinction correction, in their primary cosmology fit Perlmutter *et al.* (1999) handled extinction by performing different cuts on the supernovae, to demonstrate that the primary subset of supernovae (which omitted supernovae with significant evidence for host galaxy reddening) were not significantly affected by host galaxy reddening in comparison to the average reddening of the low-z Hamuy set of supernovae. Indeed, the comparison of the histogram and solid in in Figure 1c, which uses the U-enhanced template, would only strengthen this conclusion from Perlmutter *et al.* (1999).

4. Results and Discussion: Cosmological Parameters

Cosmological fits followed the procedure of Perlmutter *et al.* (1999). The χ^2 was calculated everywhere in a four-dimensional parameter space. The four parameters were Ω_M and Ω_L in addition to the two nuisance parameters $\mathcal{M}$, reflecting the combination of the Hubble constant and the absolute magnitude M_B of a $s = 0$ SN Ia (SHOULD I INCLUDE EQUATIONS HERE?), and α, the slope of the stretch/magnitude relationship. χ^2 was converted into probability by calculating √

$$P \propto e^{-\chi^2/2}$$

at each grid point and normalizing the over the entire parameter space. The probabilities were integrated over all values of the two nuisance parameters in order to produce the probability surface on the Ω_M/Ω_Λ plane.

Uncertainties in the fit include the magnitude uncertainties in Table 2 or 3; 1.74 (a "true" estimate of α, the stretch/magnitude slope; (Perlmutter *et al.* 1999)) times the uncertainty in s from the table, as well as the correlated error between m_B and s from the lightcurve fits; and a 300 km/s proper motion uncertainty in z (significant only for the low-redshift supernovae, where it was included in the distance modulus uncertainty). For the 42 SNe from Perlmutter *et al.* (1999), the same zeropoint covariance matrix from that paper was used as correlated uncertainties between those supernovae. For the 11 HST supernovae, we made the approximation that all of the statistical weight on m_B is due to the space based observations, and included our assumed uncertainty on the HST zeropoint (0.02) as a correlated error between those 11 SNe. To all of these these uncertainties were added an independent intrinsic supernova M_B dispersion of 0.17, and 10% of the Milkey Way extinction correction (to represent uncertainty in those values of E(B-V).)

Cosmological fits were done using four different subsets of supernovae; all four sets are based on "Case C", the primary subset of supernovae from Perlmutter *et al.* (1999). All subsets included the 16 Hamuy supernovae from Case C. Two subsets were constructed using only the Hamuy supernovae and supernovae from this paper, and two subsets were constructing adding supernovae from this paper to the full Case C set of supernovae from Perlmutter *et al.* (1999). All subsets omitted SN (9878), whose measured stretch is low enough that it would not pass the Case C criterion. For fits which do not explicitly perform E(B-V) host galaxy extinction corrections, following the procedure of Perlmutter *et al.* (1999), an additional two HST supernovae whose R-I colors were more than 3σ redder than their predicted R-I colors were omitted.

Six cosmological fits were performed to these four subsets of data; probability confidence intervals for Ω_M and Ω_L are shown in Figure 2. Table 4 lists the fits, as well as the minimum χ^2, number of data points, Ω_M and Ω_Λ in a flat universe (where $\Omega_M + \Omega_\Lambda = 1$, and $P(\Omega_L ambda > 0)$, the probability of a positive cosmological constant from the fit. (NOTE: I think I "omitted" those SNe without R-I measurements by setting their error bars to something truly huge, which means that the N and chisquare values in the table for fits (d) and (f) are probably wrong. FIX THIS.) (NOTE 2: I haven't quoted "minimum-chisquare" values of Ω's because the ellipses are actually centered left of the $\Omega_M = 0$ axis, where we didn't do the fit...!) (NOTE 3:My estimates on the flat universe values are currently extremely cheesy, and should be done better.) Fits (a) and (b) handle E(B-V) extinction in a manner identical to the Case C fit of Perlmutter *et al.* (1999): supernovae with substantial evidence for reddening are omitted. Figure 1 argues that the remaining supernovae have a residual average E(B-V) which does not differ by more than a couple of hundredths of a magnitude between the low- and high-redshift supernovae. Fits (c) through (f) explicitly correct for host galaxy extinction by subtracting $A_B = R_B E(B-V)$ from m_B for each supernova, with $R_B = 4.1$; a corresponding uncertainty $R_B \delta E(B-V)$ was added to the uncertainty on m_B for each supernova. (Those supernovae from Case C in Perlmutter *et al.* (1999) which did not have color measurements, and hence do not have direct measurements of E(B-V) were omitted from these latter fits.)

On each plot is show the Case C confidence intervals from Perlmutter *et al.* (1999), for comparison. Fits (a) and (b) are the most direct comparison, because they handled host galaxy extinction in the same manner, by omitting supernovae with evidence for significant reddening. Panel (a) demonstrates that 8 HST-observed supernovae in this sample provide a comparable constraint on Ω_M and Ω_Λ to the 42 (FIX THIS) supernovae from Perlmutter *et al.* (1999). Moreover, this independent set of supernovae produce a completely consistent cosmology to the earlier 42 supernovae. (Note, however, that both fits share the same set

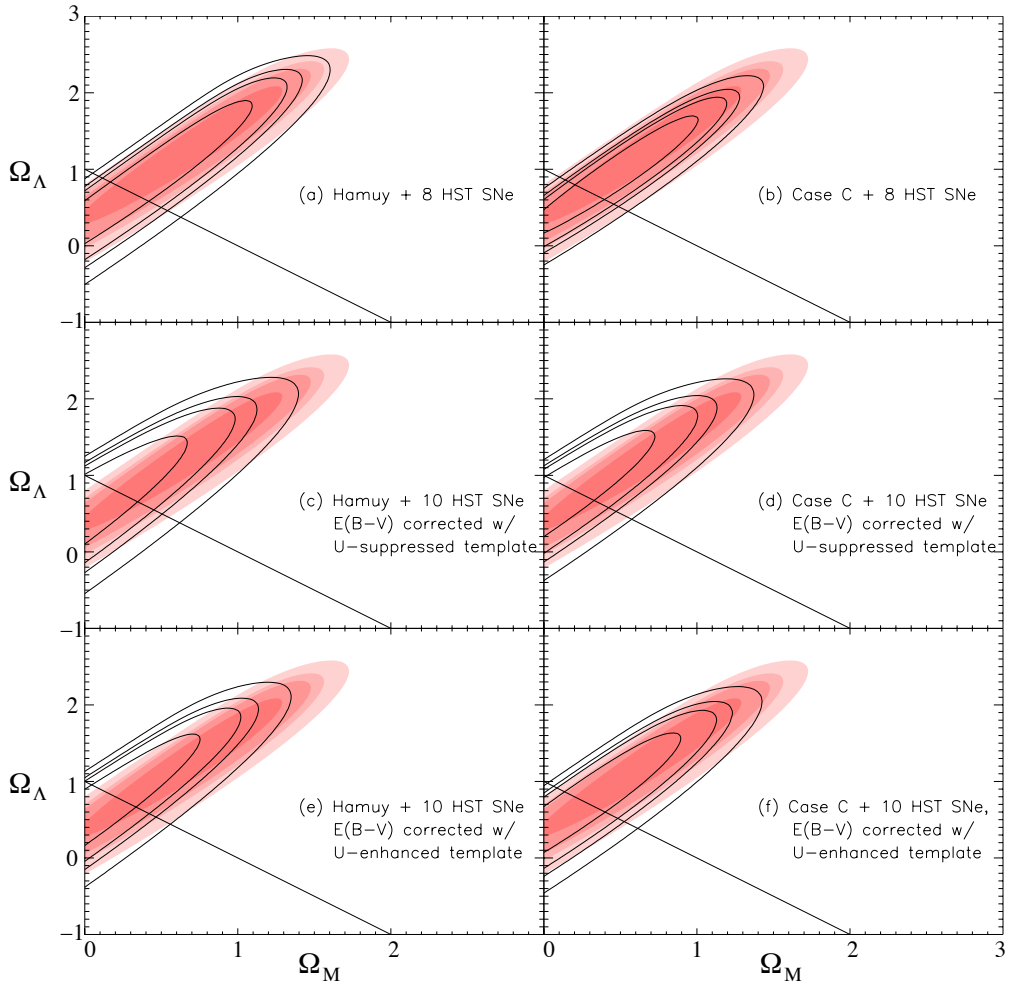

Fig. 2.— Confidence regions in the Ω_M/Ω_Λ plane resulting from χ^2 fits. In all cases, the plotted contours are 68%, 90%, 95%, and 99% confidence regions. For comparison, the primary "Case C" results of Perlmutter *et al.* (1999) are shown in solid contours on all plots. The fits on the left (a, c, and e) show the fits which include the 16 low-z supernovae from Hamuy (1996), but only the high-z supernovae from this work. The fits on the right (b, d, and f) include the "Case C" supernovae from Perlmutter *et al.* (1999). Fits (a) and (b) correct for extinction by omitting supernovae whose R-I colors are more than $3-\sigma$ redder than the predicted color. Fits (d) through (f) explicitly include E(B-V) corrections (see text). Predicted R-I colors in fits (c) and (d) came from the "U-suppressed" template, and predicted colors in fits (e) and (f) came from the "U-enhanced" template.

Table 4: Cosmological Fits

Fit	Description	N_{SNe}	Ω_M (flat)	Ω_Λ (flat)	χ^2	P($\Omega_\Lambda > 0$)
(a)	16 low-z + 8 unreddened HST	24	0.25±0.07	0.75±0.07	23.2	0.986
(b)	Case C + 8 unreddened HST	62	0.24±0.04	0.76±0.07	66.2	0.996
(c)	16 low-z + 10 HST, E(B-V) w/ U-supp. template	26	0.13±0.12	0.87±0.13	42.6	0.989
(d)	Case C + 10 HST, E(B-V) w/ U-supp. template	58	0.15±0.08	0.85±0.08	101.2	0.995
(e)	16 low-z + 10 HST, E(B-V) w/ U-enh. template	26	0.17±0.08	0.83±0.08	27.2	0.989
(f)	Case C + 10 HST, E(B-V) w/ U-enh. template	58	0.23±0.05	0.77±0.04	74.4	0.989

of 16 low-redshift supernovae.) Panel (b), which combines the data from the previous work with this data, gives the SCP's current strongest constraints on Ω_M and Ω_Λ.

Although the superior photometric measurements of the HST supernovae make them just as powerful as three four times that number of supernovae previously observed from the ground, the true value of the HST supernovae comes from their measurements of R-I, whose statistical uncertainties are much smaller than those in Perlmutter *et al.* (1999). Consequently, this allows us to include even those supernovae whose colors indicate they are reddened, and perform an explicit host galaxy extinction correction to every supernova without sacrificing too much statistical significance. These results are fits (c) through (f) in Figure 2 and Table 4. Panels (e) and (f) used E(B-V) corrections calculated from the difference between measured R-I colors and colors predicted by the U-enhanced template. As discussed in Section 3, this is the template that appears to be superior for the high-redshift supernovae. Consequently, panel (f) of Figure 2 shows what should be considered to be the primary fit for this paper which explicitly includes E(B-V) corrections. The two primary fits of the paper, panels (b) and (f), are plotted together in Figure 3 for comparison. The excellent agreement between these two fits suggest that the method of handling host extinction in Perlmutter *et al.* (1999) is good; even without explicitly factoring in E(B-V) corrections, one obtains robust cosmological results omitting those supernovae with evidence for reddening, and relying on color excess distributions to indicate that the remaining supernovae are not significantly affected by host galaxy extinction in comparison to the nearby set. Indeed, it appears that the primary effect of any bias introduced by the method of omitting those supernovae believed to be reddened is toward a closed universe, rather than either toward or away from $\Omega_\Lambda = 0$ for any given geometry. In other words, the primary effect is along the axis where the uncertainty in the supernovae results is greatest, and where the confidence regions are elongated.

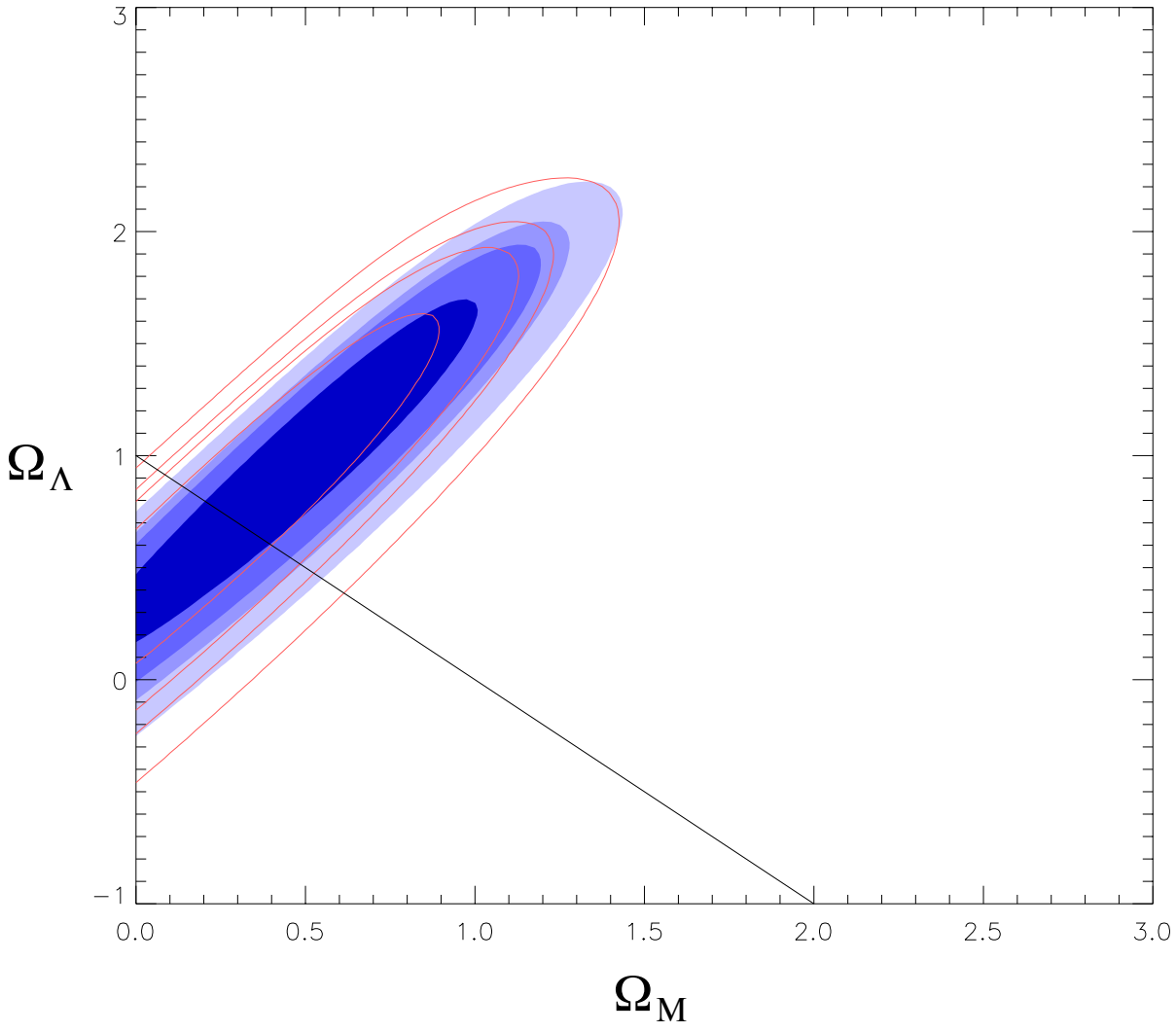

Fig. 3.— 68%, 90%, 95%, and 99% confidence regions in the Ω_M/Ω_Λ for fits (b) and (f) of Figure 2 and Table 4. Fit (b) is shown in solid contours; this fit included 8 of the HST supernovae from this paper in addition to the "Case C" supernovae of Perlmutter *et al.* (1999). Host galaxy extinction was handled by omitting supernovae with significant reddening; see Section 3. Fit (f) is shown in solid lines; this fit explicitly applied E(B-V) corrections from measured R-I colors and uncertainties, using the U-enhanced template to provide expected R-I colors for each supernova. These fits provide the strongest constraints on cosmology from SN Ia data available to date.

For fits (e) and (f), E(B-V) corrections were performed in an unbiased manner; if E(B-V) for a supernova had a negative value, then its magnitude was *decreased* as part of the color correction. A statistical distribution of E(B-V) values distributed around a value close to zero will include objects with a negative measured E(B-V); putting in a prior that reflects the physical requirement that E(B-V)> 0 biases the results, as discussed in Perlmutter *et al.* (1999). Although the E(B-V) corrections in fits (e) and (f) were unbiased, that was not the case for the fits shown in panels (c) and (d). As is apparent in Table 2, E(B-V) values are systematically very negative for supernovae at high redshifts. Because the U-suppressed template does not appear to be predicting proper values of U, these E(B-V) values are themselves biased; to "de-blue-en" supernovae by naively using them directly would produce just as biased results, especially since at the highest redshifts values of E(B-V) are negative by several tenths of a magnitude. However, it is important to estimate how much effect the use of different templates has on the calculated cosmologies. Fits (c) and (d) make the following compromise: for supernovae whose rest-B magnitudes were estimated from their observed R magnitudes (i.e. supernovae at $z < 0.7$ (CHECK THIS)), E(B-V) was used directly. For supernovae at higher redshifts, where the R-I color ☑ is more a measurement of the rest U-B color than the rest B-V color, we assumed that E(B-V) was equal to zero, plus or minus the uncertainty on the measured value of E(B-V). The values of E(B-V) calculated from the U-enhanced template for the highest redshift supernovae listed in Table 3 suggest that this assumption is approximately valid, and will produce results far less biased than negative host galaxy extinction corrections would. These results will still be biased, due to the negative values of E(B-V) for supernovae at $z < 0.7$ whose observed R magnitudes are contaminated enough by U-band light to affect their B-V color. This bias will be partially offset by the fact that the measured values of m_B will be slightly too bright by the same contamination.

A comparison of panels (d) and (f) of Figure 2 shows that there are visible differences

in the confidence regions one calculates given extinction corrections from the two different templates. However, both templates produce confidence regions which are only consistent with $\Omega_\Lambda > 0$, and the differences are less than half the width of the confidence ellipse (corresponding to a $\lesssim 1\sigma$ offset).

QUESTION: I've made it this far without showing a Hubble diagram. Will I be drawn and quartered by the cosmological community? ☑

TODO: Show a combined confidence curve which multiplies our probabilities by the CMB probabilities to produce the best SN-CMB "joint" limit on Ω_M and Ω_Λ. This means finding the "best" current published CMB confidence probability matrix. Help? ☑

5. Summary and Conclusions

The cosmological results of this study are completely consistent with those of Perlmutter *et al.* (1999). Cosmological confidence regions are calculated from an independent new set of high-redshift supernovae with high quality lightcurves produced by HST; those regions are consistent with the regions from the 42 supernovae of Perlmutter *et al.* (1999) observed from the ground. The combination of the two sets of high-redshift supernovae provide the best limits available to date on Ω_M and Ω_Λ from Type Ia supernovae. The data indicate that to extremely high probability the universe must have a positive cosmological constant. Under the assumption that the universe is flat, as is suggested by results from the Cosmic Microwave Background (REFS) the supernova data indicate that the cosmological constant has a value of XXX . The HST-observed supernova results presented in this paper have moved the minimum-χ^2 values of Ω_M/Ω_Λ closer to a flat universe than the values from Perlmutter *et al.* (1999). However, the supernova themselves do not provide a strong constraint on the geometry of the universe, as the primary elongation of the confidence ☑

ellipses in the Ω_M/Ω_Λ plane is along the axis which distinguishes a closed from a flat from an open universe. Although the error ellipses are smaller along that direction than they were in Perlmutter *et al.* (1999), a much greater number of supernovae will be required to provide a constraint on the geometry of the universe independent from the CMB measurements. Making no assumptions about the geometry of the universe, and making no assumptions about a minimum mass density, the supernova data themselves give a probability of XXX ☑ that the universe has a positive cosmological constant.

The high quality HST lightcurves in both R and I for these supernovae provide much better R-I colors than were available for the supernovae in Perlmutter *et al.* (1999). This allows us to perform direct host galaxy extinction corrections by comparing the R-I colors to an R-I color predicted from a template SN Ia spectrum, given a supernova's redshift z, lightcurve width s, and the extinction E(B-V)$_{MW}$ of the Milky Way galaxy toward the supernova. Measured colors which are redder than what is predicted indicate that the supernova suffers host galaxy extinction. While Perlmutter *et al.* (1999) had R-I measurements sufficient to determine that their supernovae did not suffer from significant host galaxy extinction *on the average*, the higher quality colors here allow us to make that determination individually for each candidate.

One result of these color comparisons is the conclusion that much better knowledge of the U-band absolute magnitude of a SN Ia will be necessary to use R-I colors to estimate E(B-V) for supernovae at higher redshifts. Our colors indicate that a template spectrum which is brighter in the U-band than has been previously assumed (but which has identical BVRI colors) better predicts the observed R-I colors. Using a "U-suppressed" template, the supernovae at higher redshifts have colors which are *too blue*, which cannot be explained by host galaxy extinction. The cosmological conclusion that $\Omega_L > 0$ is robust, however, to the use of E(B-V) corrections calculated with both U-suppressed and U-enhanced templates for

those supernovae where an estimate of the rest B-V color is available.

During the next year, two things will improve the E(B-V) measurements for these supernovae. First, it is expected that the quantity of published U-band photometry on low-redshift supernovae will greatly increase within the next year, thereby allowing us to make a better estimate of the true distribution of absolute U-band magnitudes of SNe Ia. More importantly, for a subset of these 11 supernovae we have infrared measurements made with the near infrared camera NICMOS on HST (REF BURNS), as well as with Gemini and VLT for SN2000fr (REF NOBILI?). These data are in the final stages of analysis; once they are available, the greater leverage due to the longer color baseline will provide improved estimates of host galaxy extinction.

REFERENCES

Branch *et al.*, 1996, in Canal *et al.*, eds., 1996, *Proceedings of the NATO Advanced Study Institute on Thermonuclear Supernovae*

Dolphin, 2000, PASP, 112, 1397

Hamuy *et al.*, 1996, AJ, 112, 2408

Fruchter, 2000, private communication

Goldhaber *et al.*, 2001, ApJ, 558, 359

Mielke *et al.*, 1996, MNRAS, 281, 263

Nugent *et al.*, 2002, in preparation

O'Donnell, J. E., 1994, ApJ, 422, 158

Perlmutter *et al.*1999, ApJ, 517, 586

Riess *et al.*1999, AJ, 117, 707

Schlegel, D. J., Finkbeiner, D. P., and Davis, M., 1998, ApJ, 500, 525